



Karbala International Journal of Modern Science

Manuscript 3382

Development and characterization of Sodium alginate-based active edible films functionalized with Olive Mill Wastewater Extract

Nassima HADRI

Mohamed Didi OULD EL-HADJ

Zineb MAHCENE

Fatih BOZKURT

Rusen Metin YILDIRIM

See next page for additional authors

Follow this and additional works at: <https://kijoms.uokerbala.edu.iq/home>



Part of the [Biology Commons](#), [Chemistry Commons](#), [Computer Sciences Commons](#), and the [Physics Commons](#)

Development and characterization of Sodium alginate-based active edible films functionalized with Olive Mill Wastewater Extract

Abstract

Phenolic compounds from olive mill wastewater (PCO) of Algerian origin were used to produce sodium alginate-based active films using the casting method. The effects of adding various concentrations of PCO (0%, 0.1%, and 0.2% w/v) were evaluated regarding the molecular, morphological, thermal, physicochemical, optical, barrier, biodegradability, antimicrobial, and antioxidant properties of the alginate films. The FTIR and SEM results elucidated the development of a coherent cross-linked structure attributed to hydrogen bonding interactions between PCO and alginate chains. Consequently, the films exhibited enhanced crystallinity and thermal stability, as revealed by DSC analysis. Moreover, PCO addition positively influenced several film properties, including color attributes. As the PCO concentration increased from 0% to 0.2%, significant improvements were observed in tensile strength, thickness, phenolic content, and opacity, with maximum values reaching 19.666 MPa, 0.107 mm, 80.264 $\mu\text{g/g}$, and 0.869, respectively. Additionally, the water barrier capacity and oxidative stability of sunflower oil improved significantly, with the lowest values of $0.009 \text{ kg cm m}^{-2} \text{ kPa}^{-1} \text{ d}^{-1}$ and 8.94 meq/Kg observed at a 0.2% PCO concentration. On the other hand, the film exhibited biodegradability, as evidenced by water resistance tests. The results showed that sodium alginate film coating containing PCO exhibited good anti-foodborne pathogen capacities against *E. coli*, *L. monocytogenes*, and *Salmonella enterica* with an inhibition zone between 14.6 and 19.6 mm, as well as a significant enhancement of antioxidant properties (79.506–98.682%) was observed. In conclusion, sodium alginate-based active films incorporated with PCO have demonstrated intriguing properties, making them suitable for food packaging.

Keywords

Active packaging; Food waste; Olive mill wastewater by- products; Sodium alginate.

Creative Commons License



This work is licensed under a [Creative Commons Attribution-Noncommercial-No Derivative Works 4.0 License](https://creativecommons.org/licenses/by-nc-nd/4.0/).

Authors

Nassima HADRI, Mohamed Didi OULD EL-HADJ, Zineb MAHCENE, Fatih BOZKURT, Rusen Metin YILDIRIM, Youcef RAHMANI, Aicha TEDJANI, and Muhammet ARICI

RESEARCH PAPER

Development and Characterization of Sodium Alginate-based Active Edible Films Functionalized With Olive Mill Wastewater Extract

Nassima Hadri ^{a,*}, Mohamed D.O. El Hadj ^a, Zineb Mahcene ^{a,b}, Fatih Bozkurt ^c,
Rusen M. Yildirim ^c, Youcef Rahmani ^d, Aicha Tedjani ^a, Muhammet Arici ^c

^a Kasdi Merbah University Ouargla, Natural Sciences and Life Sciences Faculty, Biological Sciences Department, Lab of Protecting Ecosystems in Arid and Semi-Arid Areas., Ouargla 30000, Algeria

^b Ecole Normale Supérieure Ouargla (ENS), Algeria

^c Yildiz Technical University, Faculty of Chemical and Metallurgical Engineering, Food Engineering Department, Istanbul 34210, Turkey

^d Scientific and Technical Research in Physicochemical Analysis (C.R.A.P.C), Algeria

Abstract

Phenolic compounds from olive mill wastewater (PCO) of Algerian origin were used to produce sodium alginate-based active films using the casting method. The effects of adding various concentrations of PCO (0%, 0.1%, and 0.2% w/v) were evaluated regarding the molecular, morphological, thermal, physicochemical, optical, barrier, biodegradability, antimicrobial, and antioxidant properties of the alginate films. The FTIR and SEM results elucidated the development of a coherent cross-linked structure attributed to hydrogen bonding interactions between PCO and alginate chains. Consequently, the films exhibited enhanced crystallinity and thermal stability, as revealed by DSC analysis. Moreover, PCO addition positively influenced several film properties, including color attributes. As the PCO concentration increased from 0% to 0.2%, significant improvements were observed in tensile strength, thickness, phenolic content, and opacity, with maximum values reaching 19.666 MPa, 0.107 mm, 80.264 µg/g, and 0.869, respectively. Additionally, the water barrier capacity and oxidative stability of sunflower oil improved significantly, with the lowest values of 0.009 kg cm⁻² kPa⁻¹d⁻¹ and 8.94 meq/Kg observed at a 0.2% PCO concentration. On the other hand, the film exhibited biodegradability, as evidenced by water resistance tests. The results showed that sodium alginate film coating containing PCO exhibited good anti-foodborne pathogen capacities against *Escherichia coli*, *Listeria monocytogenes*, and *Salmonella enterica* with an inhibition zone between 14.6 and 19.6 mm, as well as a significant enhancement of antioxidant properties (79.506–98.682%) was observed. In conclusion, sodium alginate-based active films incorporated with PCO have demonstrated intriguing properties, making them suitable for food packaging.

Keywords: Active packaging, Food waste, Olive mill wastewater by-products, Sodium alginate

1. Introduction

Over the previous few decades, biopolymer-based materials have gained considerable attention due to their role in preserving health and preventing several metabolic diseases. Therefore, the demand for eco-friendly, sustainable packaging utilizing biodegradable or compostable materials has surged in response to consumer demand for sustainability and resource rationality [1]. As defined by

Paix et al. [2], biodegradable films are flexible films manufactured from proteins, lipids, or polysaccharides, either individually or in combination, with a notable ability to rapidly decompose by microorganisms shortly after use [3]. As one of the most widely used marine polysaccharides, sodium alginate (SA) is a natural linear block copolymer composed of β-D-mannuronic and α-L-guluronic acid residues linked by a - (1–4) glycosidic bond [4]. Alginate-based films have frequently served as a

Received 7 August 2024; revised 27 October 2024; accepted 5 November 2024.
Available online 3 January 2025

* Corresponding author.

E-mail addresses: nassima.hadri@univ-ouargla.dz (N. Hadri), muarici@yildiz.edu.tr (M. Arici).

<https://doi.org/10.33640/2405-609X.3382>

2405-609X/© 2025 University of Kerbala. This is an open access article under the CC-BY-NC-ND license (<http://creativecommons.org/licenses/by-nc-nd/4.0/>).

supportive matrix for packaging materials because of their numerous advantages, such as abundant availability, low cost, non-toxicity, stability, non-immunogenicity, biodegradable properties, and exceptional abilities to emulsify and form films compared to polyethylene [5,6]. However, their limited application can be attributed to their poor ultraviolet light barrier, limited water barrier ability, and absence of antioxidant and antimicrobial activity. Given these limitations, recent investigations have focused on developing active edible films with enhanced functional attributes by incorporating other natural ingredients, such as antioxidants, antimicrobials, colorants, flavorants, or nutraceuticals [7]. Polyphenols, with their natural origin and phytochemical properties, have attracted particular interest due to their ability to generate active materials, prolong shelf life, and enhance product value [8,9]. Furthermore, since polyphenols are non-volatile compounds, they serve as an excellent alternative to essential oils, helping to minimize the potential negative effects of essential oils on the sensory properties of food and their tendency to volatilize during extended storage [10,11]. In this context, several studies conducted by Aloui et al. [12], Chen et al. [13], and Dou et al. [14] proved that the incorporation of gallnut extract, thymol extract, and tea polyphenols into sodium alginate composite films was able to satisfy antioxidant and antibacterial capacity as well as improve the mechanical and barrier properties of the film, respectively. On the other hand, the high costs associated with olive processing residues in Mediterranean countries have prompted the development of eco-friendly methods for recovering and enhancing olive byproducts in food packaging, leveraging their rich nutritional content, value-enhancing additives, and bioactive compounds. In this regard, the previous study by Zam, W [15] demonstrated the effectiveness of incorporating olive leaf extract in conjunction with chitosan or alginate to improve the physicochemical attributes of sweet cherries. This combination ensured the optimal retention of phenolic compounds and delayed the ripening process of sweet cherries compared to uncoated fruit samples. Likewise, Ng and Tan [16] stated the performance of the aqueous olive extract hydroxytyrosol in enhancing both the barrier properties and mechanical attributes of the film when incorporated into alginate bilayer films.

Olive mill wastewater is a liquid byproduct produced during the extraction of olive oil. It is often released into the aquatic environment without treatment. The olive mill wastewater produced during milling typically ranges from 0.5 to 1.5 m³ per 1000 kg of olives. The main characteristics of

olive mill wastewater include a high concentration of suspended solids (1–9 g L⁻¹), low pH (3 < pH value < 5.9), and high chemical oxygen demand (COD: 45–170 g L⁻¹, BOD₅: 35–110 g L⁻¹), along with other recalcitrant organic compounds (52270–180 000 mg L⁻¹ Pt–Co units) [17]. The uncontrolled release of untreated olive mill wastewater poses significant environmental damage due to its phytosanitary and antimicrobial effects. Traditional methods of treatment for olive mill wastewater involve physicochemical processes (flocculation, coagulation, and adsorption), advanced oxidation processes, membrane treatment (such as ultra-filtration, reverse osmosis, micro-filtration), biological treatments (aerobic and anaerobic digestion), or combined processes [17] have been proposed to mitigate the harmful impact of olive mill wastewater. Despite their effectiveness, these methods face limitations such as high costs, technical complexity, and pollutant emissions. Alternatively, recent research highlights the potential of olive mill wastewater as a raw material for producing industrial products, including bioactive compounds, enzymes, biofuels, biopolymers, and single-cell proteins. Olive mill wastewater is rich in phenolic compounds, such as simple phenols, secoiridoids, flavonoids, and lignans, which are known for their potent antioxidant and antimicrobial activity. The concentration of phenolic compounds in olive mill wastewater varies significantly from 0.5 to 24 g L⁻¹ [17]. These phenols are too valuable to be diminished or discharged into the environment. Consequently, the bio-based recovery of olive mill wastewater through the extraction of phenols and their integration into biodegradable packaging films could improve the performance of packaging systems and prolong the shelf life of food products. This approach presents an opportunity for recycling and a sustainable solution for managing olive mill wastewater. Based on the literature, the residual organic matter in olive mill wastewater can be transformed into carbon composites, which can then be used to eliminate emerging pollutants. The proposed strategy offers a dual approach for valorizing these wastes and also opens new avenues for applications by integrating bioactive phenolic compounds into active packaging.

Despite many researchers demonstrating the performance of bioactive compounds from olive byproducts, mainly olive leaves and pomace, when incorporated into film-forming formulations to improve barrier and mechanical film properties and to extend food shelf life, their effects on the functional properties of food packaging materials have not been fully elucidated.

To the best of our knowledge, there are no studies in the literature related to the incorporation of phenolic compounds from olive mill wastewater into biodegradable packaging films and their characterization. Therefore, the present study aims to develop a novel sodium alginate (SA) edible film by incorporating different concentrations of phenolic compounds extracted from Algerian olive mill wastewater (PCO) for use as an alternative to non-biodegradable films for food preservation. The effects of PCO incorporation into the resulting composite films on bioactive properties, such as moisture content, thickness, barrier protection, mechanical, thermal, molecular, microstructure, optical, biodegradability, antioxidant, and antibacterial properties, were evaluated.

2. Materials and methods

2.1. Material and extraction process

For this study, fresh olive mill wastewater samples from Chemlal cultivars were obtained from a continuous chain oil mill in southern Algeria. The samples were collected in sealed plastic containers and promptly cooled before being transported to the laboratory, where they were kept at a temperature of 4 °C for subsequent analysis. The extraction of phenolic compounds was achieved using the method described by De Marco et al. [18]; liquid–liquid extraction using ethyl acetate was performed. Initially, olive mill wastewater was acidified with HCl and subsequently washed with hexane. The phases were separated when the washed olive mill wastewater samples were combined with ethyl acetate (10 mL, v/v). The extractions were performed three consecutive times at 25 °C. At 40 °C, a rotary evaporator was used to evaporate the ethyl acetate. The dry residue of the polyphenol extract was frozen at –20 °C until utilization.

2.2. Individual phenolic compounds analysis by HPLC

A High-Performance Liquid Chromatography (HPLC) system (LC-20AD pump, SIL-20A HT autosampler, CTO-10ASVP oven, DGU-20A5R degasser, CMB-20A communication module) connected to a diode array detector SPDM20A DAD (Shimadzu, Japan) was used to identify the composition of phenolic compounds. The analysis followed the method described by Capanoglu et al. [19]. A GL Sciences Inertsil ODS-3 (25 cm × 4.0 mm, GL Sciences, Tokyo, Japan) 5 µm column with an Inertsil ODS-3 cartridge guard column (4.0 × 10 mm, GL

Sciences, Tokyo, Japan) was employed. The column temperature was maintained at 40 °C, and the detection of phenolic compounds was executed at 278, 325, 236, 254, and 517 nm wavelengths at a flow rate of 1 mL/min. The mobile phase consisted of A: ultrapure water containing 0.1% (v/v) trifluoroacetic acid and B: acetonitrile containing 0.1% (v/v) trifluoroacetic acid.

2.3. Film preparation

Sodium alginate-based films (SA) were prepared by dissolving 2 g of SA with 40% (w/w) glycerol in 100 mL of distilled water. The resulting sodium alginate film-forming solution (SFS) was then heated at 70 °C for 1h. Different concentrations of PCO (0%, 0.1%, and 0.2% (w/v)) were added to the polymer solutions after the SFS was cooled to room temperature. The resulting film-forming solutions were degassed using ultrasonication, separated into 18 g portions in Petri dishes, and dried at 40 °C for 24 h in an incubator.

2.4. Chemical characterization by FTIR analysis

A Fourier Transform Infrared (FTIR) instrument (Bruker Tensor 27 spectrometer equipped with a DLa TGS detector, Bremen, Germany) was used for spectral analysis to elucidate the structural interactions and functional groups in the produced films. The FTIR measurements were conducted in the 4000 to 400 cm⁻¹ spectral range [20].

2.5. Scanning electronic microscopy analysis

The surface morphology of the film samples was analyzed using scanning electron microscopy (SEM) (Thermo Fisher Apreo 2 S FEG-SEM, EU). The films were placed on aluminum stubs using carbon tape with an Au coating. They were then examined using an accelerating voltage of 10 kV. Chemical characterization was performed using FTIR analysis.

2.6. Thermal properties

The Differential Scanning Calorimetry instrument (DSC Q20, TA Instruments, Inc., USA) was used for thermal analysis of the film samples to evaluate their endothermic and exothermic properties. Precisely, 5 mg samples were weighed into an aluminum pans, sealed with an aluminum lids, and then heated at 10 °C/min from 30 to 400 °C under a nitrogen stream. An empty aluminum pan was used as a reference.

2.7. Film thickness and moisture content

A digital micrometer (Fowler Digitrix Mark 2, Chicago, USA) was used to measure the thickness of the film samples. Five measurements were taken from different points on each sample to determine the average value. According to Ciannanea et al. [21], the oven-drying method was used to measure the moisture content of the films. To achieve equilibrium weight, film samples weighing 1–3 g were dried for 24 h at a temperature not exceeding 105 °C. Afterward, the weight of the dry samples was subsequently determined.

2.8. Thermal properties

The water vapor permeability (WVP) of the films was determined based on the methods described by Liu et al. [22]. For this purpose, cells filled with thoroughly dried silica gel were sealed with the film sample and placed in a controlled relative humidity (90% RH) and temperature (30 °C) chamber. The weight change of the cup was recorded at 2 h intervals throughout the day. Non-film silica gel cells were used as controls. From the following Eq. (1), the WVP has been estimated:

$$WVP = W X / t \Delta p A \quad (1)$$

Where: WVP: water-vapor permeability; w/t: mass change over time in g; t: time in h; X: thickness in mm, Δp : partial vapor pressure difference between atmosphere and sample cell (2642 Pa) at 24 °C and A: film area in m^2

The methodology outlined by Memis et al. [23] was employed to measure the oxygen permeability ($O_2 P$) of the films, with minor adaptations. A film sample was precisely cut and affixed to the opening of a conical flask containing 15 mL of antioxidant-free sunflower oil. The samples were then incubated at 80 °C for 9 days. Results were obtained using sodium thiosulfate titration at three-day intervals.

2.9. Optical properties

A chromameter (CR-400 Konica Minolta Sensing, Inc., Osaka, Japan) was utilized to measure the optical properties (L^* , for black to white; a^* , for red to green, and b^* , for yellow to blue) of the films. Five measurements at least were taken for each film sample, as described in a prior study by Tornuk et al. [20].

The opacity of the films was determined by measuring their absorbance at 600 nm using a UV

spectrophotometer (Thermo Scientific GENESYS 20, Thermo Fisher Scientific, Inc., and Rochester, NY, USA). Following the method described by Park et al. [24], the films were immediately placed in a spectrophotometer test cell after being sliced into rectangles. An empty test cell was utilized as a reference. Using the following Eq. (2), the opacity of films was determined.

$$T = \text{Abs}600/d \quad (2)$$

Where T is the transparency, Abs600 is the value of absorbance at 600 nm, and d is the film thickness (mm).

2.10. Mechanical properties

The films were prepared according to the ASTM D882-12 standard procedure [25] and sliced into rectangular pieces of 7 cm \times 2 cm for tensile strength (TS) and elongation at break (E %) tests. At least five replications for each sample were tested using a texture analyzer (TA.XT Plus, Stable Micro Systems, Surrey, UK) fitted with a 100 kg load cell. The grip distance and crosshead speed were set at 50 mm and 4 mm/s, respectively.

2.11. Swelling index (SW)

The water resistance of films was assessed using the swelling test, following the method described by Yoon et al. [26], with a minor modification. Film samples (2 mm \times 2 mm) were weighed (W_0) before being soaked in distilled water for 24 h. Each sample was then carefully delicately wiped with tissue paper and weighed (W_t). In this sense, the following equation was used to determine the swelling percentage

$$\text{Swelling (\%)} = (W_t - W_0) / W_0 \times 100 \quad (3)$$

Where W_0 is the initial mass of the sample film (g) and W_t is the mass of the sample film (g) at time t (h).

2.12. Water solubility (WS)

To determine the water solubility (WS) of film samples, pieces of film measuring 1 \times 3 cm^2 were dried at 100 °C for 24 h to determine the initial dry matter. After being soaked in 50 mL of distilled water for 24 h at 25 °C, these samples were dried in the oven at 24 h at 100 °C to determine the final dry matter. According to Dutta et al. [27], the WS was

reported as the difference between the initial and final dry matter weight.

$$\text{WS \%} = \frac{(\text{Initial dry weight} - \text{Final dry weight})}{\text{Initial dry weight}} \times 100 \quad (4)$$

2.13. Total phenolic assay

The total phenolic content (TPC) of the prepared films was determined using Folin's phenol reagent. To this end, 2.5 mL of the film extract was mixed with 0.3 mL of Folin-Ciocalteu reagent (10% v/v) and 2 mL of a 7.5% (w/v) sodium carbonate solution. After incubating the mixture in the dark at room temperature for 5 min, the absorbance was measured using a UV–vis spectrophotometer. A calibration standard was prepared using a gallic acid solution. The TPC value of each film was expressed as mg gallic acid equivalent per gram of film.

2.14. Determination of antioxidant activity

The antioxidant activity of the films was evaluated by measuring their ability to scavenge free radicals using 2,2-diphenyl-1-picrylhydrazyl (DPPH). Briefly, 1.5 mL of the ethanol extract was combined with 0.5 mL of a 0.1 mM ethanolic DPPH solution. The resulting mixture was kept in the dark for 60 min at ambient temperature. Finally, the absorbance of the DPPH assay mixture was measured at 517 nm using a UV–visible spectrophotometer. The DPPH (%) scavenging activity was calculated using the following formula (Eq. 5):

$$\% \text{DPPH scavenging} = \frac{(A_{\text{Control}} - A_{\text{sample}})}{A_{\text{Control}}} \times 100 \quad (5)$$

Where, A_{Control} represents the absorbance of the control, while A_{sample} represents the absorbance of the sample.

2.15. Determination of antimicrobial activity

The antibacterial efficacy of the produced films against *Escherichia coli*, *Staphylococcus aureus*, *Listeria monocytogenes*, and *Salmonella enterica* was evaluated using the agar diffusion method. A 100 μL aliquot of the test strain (1.5×10^8 CFU/mL) was evenly spread on nutrient agar plates. Circular discs with a 10 mm diameter were sliced from the films and placed onto the respective plates. The plates were then incubated at 37 °C for 24 h. The results were determined by measuring the diameter of the translucent halo (mm) surrounding the films. All experiments were performed in triplicate.

2.16. Statistical analysis

All the collected data were analyzed using an analysis of variance (ANOVA), followed by multiple comparisons using the Tukey test, at a significance level of 95%. The SPSS statistical computer software package (IMB SPSS 25) was employed in this study.

3. Results and discussion

3.1. Individual phenolic composition of PCO

HPLC analysis was carried out to estimate the content of the main phenolic compounds in PCO (mg/mL). As shown in Table 1, several components were detected at wavelengths of 278, 325, 236, 254, and 517 nm. The main phenolic compounds in the PCO extract were hydroxytyrosol (446.85 mg/L) and tyrosol (167.4 mg/L). These compounds have attracted attention due to their potent antioxidant activity [28]. Moreover, they are associated with various biological activities, including antimicrobial, anti-carcinogenic, and anti-inflammatory effects [29]. Other phenolic compounds found in residual amounts include catechin, vanillic acid, caffeic acid, ferulic acid, sinapic acid, p-coumaric acid, protocatechuic acid, and chlorogenic acid. The phenolic profile of olive mill wastewater was found to be substantially close to that reported in previous studies [30–32]. However, the identified phenolic compounds in olive mill wastewater and their respective concentrations exhibit variability across different studies, as comprehensively reviewed by Obied et al. [33].

In general, it can be concluded that the content and composition of phenolic compounds in olive mill wastewater depend on a multitude of factors, including the fruit (e.g., cultivar, maturity), climatic

Table 1. Major phenolic compounds concentration of PCO (mg/L).

Phenolic Compounds	Retention Time (min)	Concentration (mg/L)
Hydroxytyrosol	9.900	446.85
Tyrosol	14.154	167.4
Catechin	11.985	126.95
Vanilic acid	18.086	62.3
Protocatechuic acid	8.832	49.5
3-Hydroxybenzoic acid	19.034	48.8
Myricetin	26.645	43.5
Quercetin	32.862	27.6
Caffeic acid	14.661	7.17
Rutin	27.857	9.85
Phloridzin	35.580	22.52
Syringic acid	15.389	6.235
Elagic acid	20.297	15.375
Chrysin	41.247	6.36
4-Hydroxybenzoic acid	15.393	14

conditions, storage duration, malaxation time, and the milling process [33].

3.2. Chemical characterization by FTIR analysis

FTIR spectroscopy was carried out to identify the functional groups and analyze intermolecular interactions between the SA matrix and PCO based on the specific positions and intensities of the distinctive absorption peaks observed. As shown in Fig. 1, the FTIR spectrum of alginate film is consistent with those previously reported by Khaoula Khwaldia et al. [34], Abdin et al. [35], and Luo et al. [36]. It exhibits characteristic bands at 3275, 2926, 1600, 1406, and 1026 cm^{-1} , corresponding to $-\text{OH}$ groups, C–H stretching, asymmetric COO^- stretching, symmetric COO^- stretching, and C–O–C stretching, respectively. According to Augusto et al. [37], the peak at 896 cm^{-1} in the alginate film spectrum indicates the presence of mannuronic acid residues. Additionally, the peak at 817 cm^{-1} is characteristic of these residues, while the band at 948 cm^{-1} corresponds to the C–O stretching vibration of uronic acid residues. The addition of PCO resulted in a significant reduction in the intensity of the alginate characteristic bands, indicating a strong interaction between PCO and the SA polymer. Specifically, the absorption bands of O–H groups, asymmetric COO^- stretching, and symmetric COO^- stretching decreased and shifted to lower frequencies (3275 cm^{-1} , 1600 cm^{-1} , and 1403 cm^{-1} , respectively). Additionally, a new peak at 1727 cm^{-1} , corresponding to the C=O stretch in the composite film, confirms the presence of PCO and indicates cross-linking [38]. Our FTIR results are consistent with those obtained by Júnior et al. [39]. These findings support that alginates interact with

PCO mainly through the formation of intermolecular hydrogen bonds involving the hydroxyl and COO^- groups of alginate and the hydroxyl groups of polyphenols [40].

3.3. Film thickness and moisture content

A notable enhancement in film thickness was observed with the increase in PCO extract ($p > 0.05$, Table 2), from 0.093 ± 0.004 mm to 0.107 ± 0.005 mm. This outcome suggests that the PCO extract either altered the films' solid content or interfered with the formation of biopolymer networks. Moura-Alves [41] previously reported consistent findings, noting a thickness of 63.67 μm for sodium alginate films, which increased to 137.37 μm for films enriched with olive leaf extract. The moisture content of neat SA films was 10.04% (Table 2). Adding PCO at 0.2% decreased the moisture content of the films to a minimum of 7.88%. This reduction may be attributed to interactions between PCO and the SA film matrix, which could have promoted hydrogen bonding and hydrophobic interactions, leading to more tightly packed films. As a result, the films' water absorption capacity was reduced, thereby decreasing their moisture content.

3.4. Color and opacity of films

The optical properties data for the sodium alginate films and composite films are presented in Table 2. The pure film exhibited high clarity and translucence, as demonstrated by its highest L^* value (88.18 ± 0.27) and lower opacity (0.69 ± 0.07). However, the addition of PCO resulted in decreased transparency values for the alginate films ($p < 0.05$),

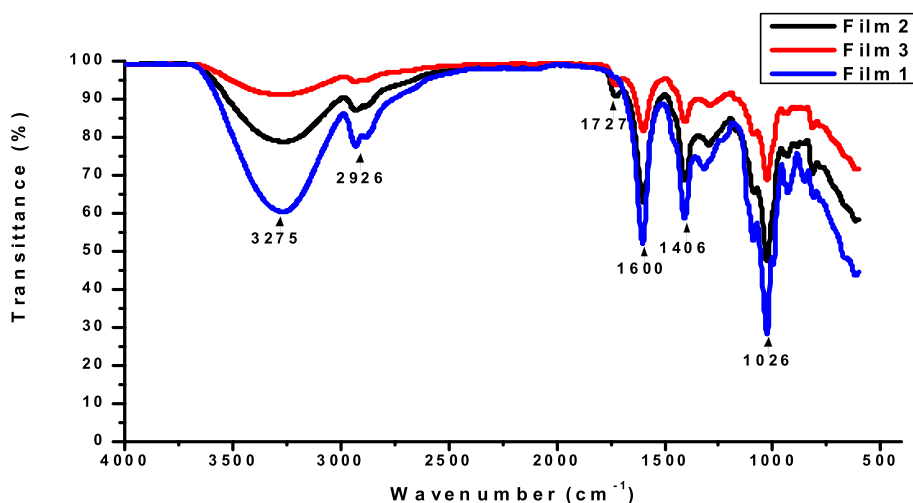


Fig. 1. Fourier transform infrared spectrum of the films. Film 1: pure SA film; Film 2: composite SA film fitted with 0.1% of PCO; Film 3: composite SA film fitted with 0.2% of PCO.

Table 2. Thickness, percent moisture, color, opacity values of the film samples.

Film sample	Thickness (mm)	Moisture %	Color				Opacity
			L*	a*	b*	ΔE	
Film 1	0.093 ± 0.004 ^(c)	10.048 ± 0.714 ^(a)	88.187 ± 0.279 ^(a)	-0.7 ± 0.148 ^(a)	4.347 ± 0.616 ^(b)	5.766 ± 0.236 ^(b)	0.692 ± 0.070 ^(b)
Film 2	0.101 ± 0.002 ^(ab)	8.673 ± 1.847 ^(a)	85.51 ± 0.305 ^(b)	-0.843 ± 0.032 ^(a)	6.747 ± 0.178 ^(a)	8.521 ± 0.329 ^(a)	0.762 ± 0.042 ^(ab)
Film 3	0.107 ± 0.005 ^(a)	7.884 ± 0.885 ^(a)	84.937 ± 0.339 ^(b)	-0.747 ± 0.028 ^(a)	5.307 ± 0.198 ^(b)	8.952 ± 0.999 ^(a)	0.869 ± 0.012 ^(a)

ΔE : Total color difference. a-c: Lowercase letters within the same line refers to statistically significant differences ($P < 0.05$). Film 1: pure SA film; Film 2: composite SA film fitted with 0.1% of PCO; Film 3: composite SA film fitted with 0.2% of PCO.

with significant reductions in L* values to 85.51 and 84.93 for the films containing 0.1% and 0.2% PCO, respectively. This reduction suggests less light reflection from the film surfaces. The addition of PCO caused the films to exhibit a high tendency towards yellowness, as confirmed by the elevated b* value ($p < 0.05$). This increase in yellowness could be ascribed to the characteristic brown color of the PCO. Moreover, the inclusion of PCO significantly affects the appearance of the films, as indicated by the higher ΔE values, which increased from 5.76 ± 0.23 to 8.95 ± 0.99 compared to the neat SA films. As stated by Kuan et al. [42], the addition of mulberry leaf extract to sodium alginate films led to a decrease in the L* value and an increase in the b* value and total color change (ΔE), which aligns with the findings of the present work. In a similar vein, Oliveira Filho et al. [43] highlighted that darker packaging materials with higher opacity percentages are employed for fatty foods to prolong their shelf life. This approach minimizes the light's direct contact with the food, thereby preventing the catalytic effect on lipid oxidation and contributing to its preservation. Therefore, the resulting films might delay the lipid oxidation of food due to their low transmittance.

3.5. Surface morphology

The SEM micrographs of the surface morphology of the developed films are shown in Fig. 2. The pure sodium alginate film exhibited a smooth and homogeneous microstructure with some irregularities, including a few cracks and holes, likely due to foreign materials and coating substances. After incorporating PCO, notable changes in surface morphology were observed. Specifically, the composite films exhibited fewer cleavages and displayed a more continuous and smoother surface with reduced visible cracks and pores. This suggests effective integration of the PCO extract into the SA matrix. The improved surface morphology indicates a high compatibility between PCO and SA, likely facilitated by intermolecular hydrogen bond formation, as corroborated by the FTIR analysis. These morphological enhancements, resulting from the

successful dispersion of PCO within the alginate matrix, align with the observed improvements in barrier properties and mechanical strength. The reduced surface defects and increased smoothness likely contribute to the enhanced performance of the films.

3.6. Thermal properties

The thermal behavior properties of film samples were evaluated by DSC analysis, as displayed in Fig. 3. The DSC analysis of the pure SA edible film revealed a distinctive curve with two peaks. The first endothermic peak was observed at 119.77 °C, indicating a phase transition associated with melting and potentially related to the elimination of loosely bound water. The second exothermic peak, at 209.40 °C, corresponded to the subsequent decomposition of the sample. Comparatively, incorporating PCO extract into SA films significantly enhanced the thermal stability of the composite films. The film samples containing PCO exhibited higher values of ΔH_m , T_m , and T_d compared to the pure film (Table 3).

This behavior suggests that the interaction between SA and the PCO extract, through increased hydrogen bond formation with higher PCO content, effectively suppressed the mobility of the SA chains, resulting in improved thermal stability of the films. According to Martins et al. [44], changes in thermal stability are often related to the crystallinity of the film samples, where a higher degree of crystallinity corresponds to higher thermal stability due to the increased energy (heat) required to disrupt a more crystalline structure. The study revealed that the increasing crystalline degree of the films corresponded with their enhanced thermal stability. As the PCO extract concentration increased, the SA films became more crystalline due to interactions between the PCO and SA matrix, resulting in improved stability compared to films without PCO. Similar improvements in thermal stability with the addition of other compounds have been observed by Júnior et al. [45], who noted enhanced stability in SA films with tannic acid, and Li et al. [46], who reported similar effects with hydrolyzed collagen.

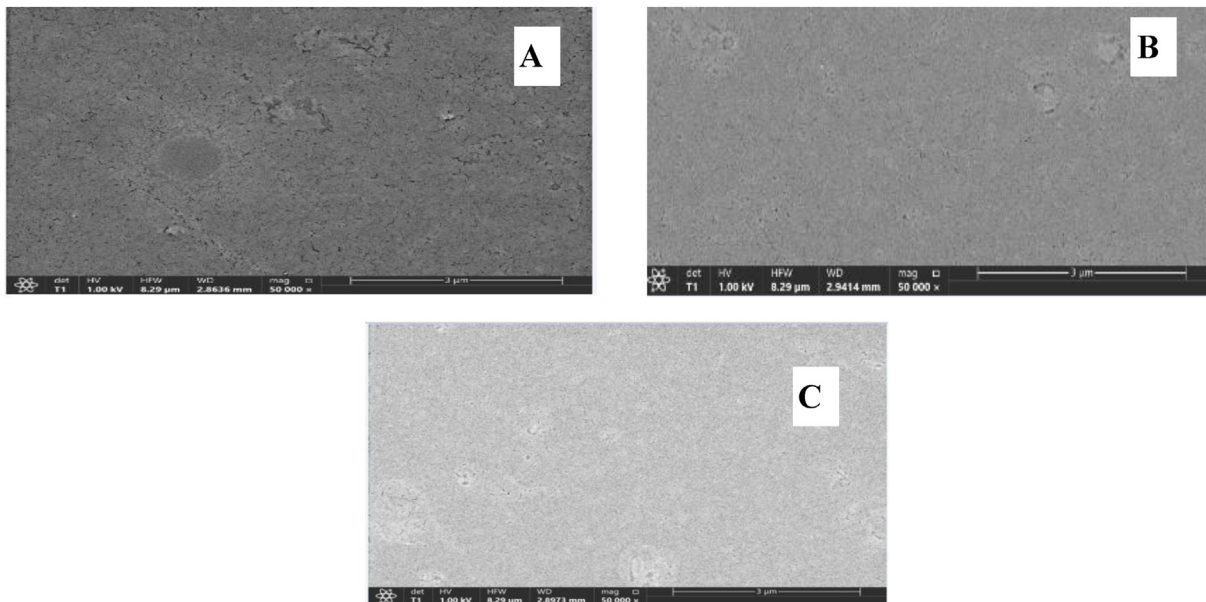


Fig. 2. Scanning electron microscopy (SEM) micrographs of surface (magnification: 50000 \times). A: pure SA film; B: composite SA film fitted with 0.1% of PCO; C: composite SA film fitted with 0.2% of PCO.

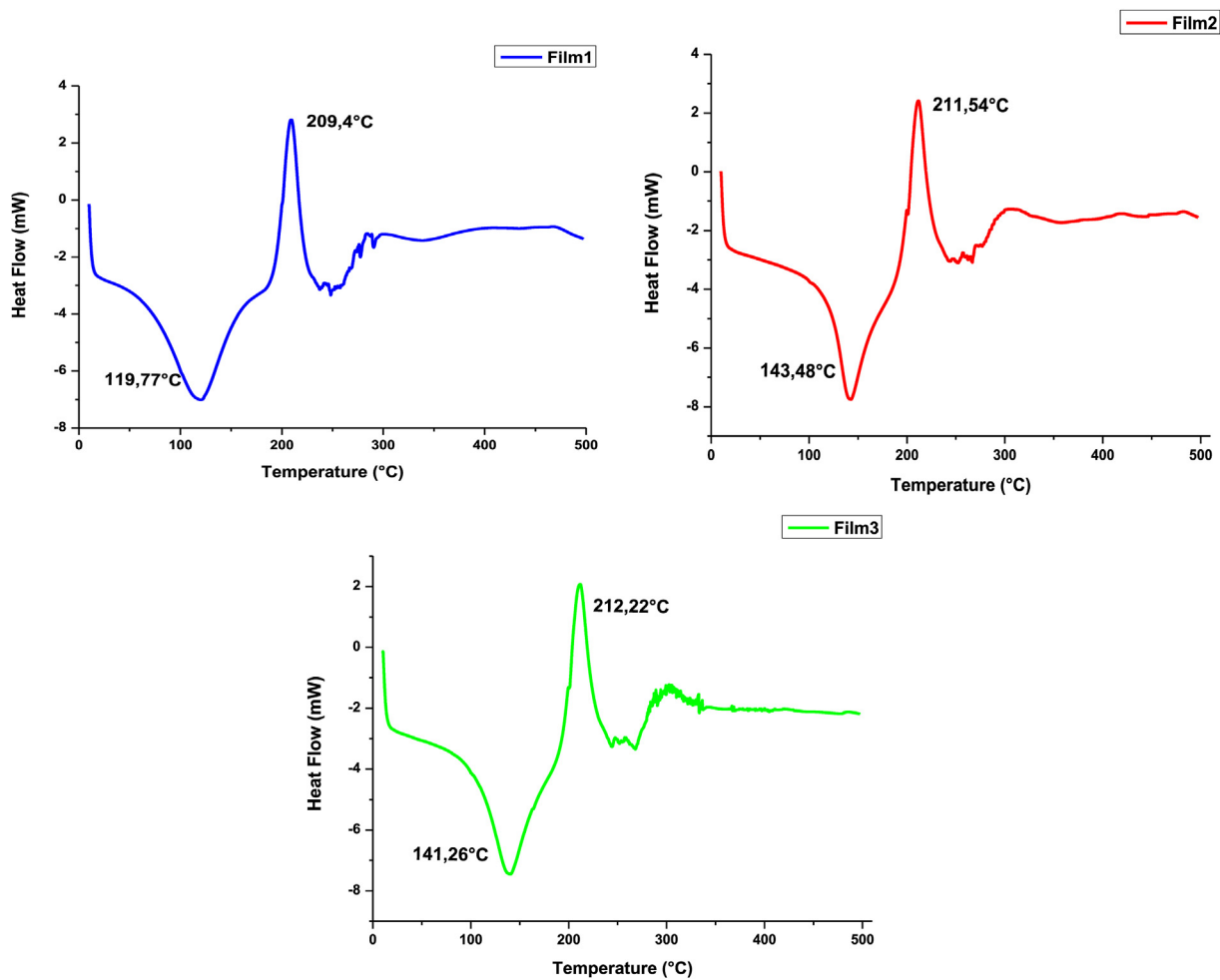


Fig. 3. DSC thermograms for the studied films. Film 1: pure SA; Film 2: composite SA film fitted with 0.1% of PCO; Film 3: composite SA film fitted with 0.2% of PCO.

Table 3. Calorimetric, water vapor permeability, water solubility and swelling values and mechanical proprieties of the film samples.

Film sample	DSC analyses			Mechanical proprieties		WVP (kg cm m ⁻² kPa ⁻¹ d ⁻¹)	SW %	WS %
	T _m (°C)	Δh _m (J g ⁻¹)	T _d (°C)	Elongation (%)	Tensile strength (MPa)			
Film 1	119.77	299.6	209.40	2.26 ± 0.884 ^(a)	11.703 ± 2.675 ^(b)	0.011 ± 0.001 ^(b)	/	/
Film 2	143.48	319.6	211.54	2.22 ± 0.113 ^(a)	12.156 ± 1.387 ^(b)	0.010 ± 0.000 ^(bc)		
Film 3	141.26	383.7	212.22	1.845 ± 0.551 ^(a)	19.666 ± 1.453 ^(a)	0.009 ± 0.000 ^(c)		

T_m: melting temperature; Δh_m: enthalpy of melting; T_d: temperature of decomposition; WVP: Water Vapor Permeability; SW: swelling index; WS: water solubility. a-c: Lowercase letters within the same line refers to statistically significant differences (P < 0.05). Film 1: pure SA film; Film 2: composite SA film fitted with 0.1% of PCO; Film 3: composite SA film fitted with 0.2% of PCO.

3.7. Mechanical properties

Protecting the internal integrity of food requires an understanding of packaging behavior against stress applied to its surface, which is related to the mechanical properties of the packaging films. Tensile strength (TS) represents the mechanical strength of the film, while elongation at break (E %) measures its plasticity, which is the capacity of a film to extend before breaking. The results of mechanical strength and E% for all the prepared films are illustrated in Table 3. The addition of PCO distinctly influenced the mechanical properties. The tensile strength of the pure sodium alginate was 11.703 ± 2.67 MPa, whereas, with the increase in the PCO content, TS significantly (P < 0.05) increased to 19.666 ± 1.453 MPa. It has been stated that the composition and processing techniques used influence the interactions between molecules, which in turn determine the mechanical properties of composite films. Based on our results, the effect of the extract on the mechanical properties of the film may be attributed to the fact that PCO has been well dispersed in the SA matrix without any aggregation and has effectively crosslinked the film matrix. As a result, strong interfacial interactions between the PCO extract and the sodium alginate matrix were produced through intermolecular hydrogen bonding, resulting in a more compact structure. Consequently, the tensile strength of the composite films was enhanced. In terms of elongation at break, the addition of PCO extract did not result in a statistically significant (P > 0.05) impact on the SA-based film's elongation at break values. This outcome can be attributed to the degree of crosslinking produced, which, although significantly increased the film's tensile strength was insufficient to affect its plasticity.

3.8. Vapor permeability (WVP) of films

The shelf life of food products is directly related to the transfer of water between the preservative films and the surrounding environment. As shown in

Table 3, a notable reduction (p < 0.05) in water vapor permeability (WVP) was observed with an increase in PCO extract. The hydrophilic/hydrophobic ratio of the film is crucial since water transmission often occurs through the hydrophilic portion of the packaging. The addition of PCO extract resulted in an enhancement of the WVP of the films. This improvement can be attributed to the increased hydrophobic properties of the films. It is also suggested that strong interfacial interactions between the phenolic compounds and the biopolymers could lead to the formation of a denser composite film system, consequently contributing to improved water barrier properties [47,48]. Similar results have been obtained by Yoshida et al. [49] and Wu et al. [48], who reported that the positive influence in WVP values of the composite films was attributed to the dense structure established through intermolecular interactions between polyphenols and biopolymers.

3.9. Swelling degree and water solubility

The water resistance of films was measured in terms of swelling (SW) and solubility in water (WS), as shown in Table 3. All films were almost completely dissolved in water and disintegrated during immersion in water, which made it impossible to measure the SW and the WS. The solubility of edible film is determined by the hydrophilic and hygroscopic properties of film-forming compounds. The research conducted by Costa et al. [50] highlights that the water solubility of sodium alginate, along with its abundance of hydroxyl groups and lower concentration of carboxylic acid groups, promotes the formation of intermolecular hydrogen bonds. The low water resistance of the films can be attributed to the lower concentration of PCO extract, which is insufficient to significantly enhance film resistance. Although the PCO extract contributes to forming a compact structure, SA composite films still have strands that can absorb water, leading to high values of swelling index and water solubility. Looking at these results, the high swelling capacity

and solubility of film samples may be a contributing factor to their rapid biodegradability and ease of digestibility. Consequently, one proposal is to use SA films enriched with PCO extract for food products designed to undergo melting during cooking, serving as coatings or wraps for various meat products. Additionally, these films could also function as absorbent pads within meat packages, creating an effective barrier against oxygen and moisture.

3.10. Peroxide values of sunflower oil

Fig. 4 illustrates the film samples' oxygen permeability (O_2P), measured in terms of peroxide value. Throughout the experiment, the control oil had the highest peroxide value of 11.84 ± 0.11 meq/Kg, attributable to the direct exposure of sunflower oil samples to external oxygen. In contrast, sunflower oil protected by SA film containing 0.2% PCO extract exhibited the lowest O_2P (8.94 ± 1.29 meq/Kg). All samples showed a significant increase in O_2P of sunflower oil stored at 80°C over 9 days compared to the initial value. However, the continuous pattern of increase for samples protected with SA film containing PCO was slower. It was reported by Sothornvit and Pitak [51] that hydrophilic biopolymer films exhibited excellent oxygen barrier. Additionally, incorporating PCO extract into SA films enhances their antioxidant abilities, as demonstrated by the outcomes of the DPPH radical scavenging activity and TPC. This enhancement potentially slows the oxidation of the oil and improves the barrier properties. Moreover, the SA composite films displayed a more compact structure compared to pure SA films, as indicated by the DSC results (Table 3) leading to improved barrier properties. Based on the obtained results, SA film

containing PCO can effectively protect food with high oil content from unfavorable oxidation reactions, which initiate several food changes such as odor, color, flavor, and nutrient deterioration.

3.11. Total phenolic content (TPC)

Polyphenolic-enriched extracts have recently gained more attention due to their bioactive properties. The results of adding PCO to the total phenolic content of film samples are presented in Table 4. As observed, the TPC of pure SA films was $64.37 \mu\text{g} \pm 0.005$ GA equivalent/g film due to the phenolic groups naturally present in alginate [52]. Notably, The TPC significantly increased ($p < 0.05$) with higher PCO content, reaching a maximum of $98.682 \pm 0.285 \mu\text{g}$ GAE/g film for films with the highest PCO content (0.2%). This increase in TPC is directly correlated with the rise in overall phenolic content in SA films enriched with PCO extract. This elevated TPC in the SA composite films is attributed to the phenolic acids present in the PCO composition, which reacted with the Folin–Ciocalteu reagent [53]. Santos et al. [54] observed similar findings, reporting an increase in total phenolic content (TPC) in sodium alginate films with the addition of purple onion peel extracts.

3.12. Antioxidant activity of films

The antioxidant activity of film samples was evaluated to test the ability of films to act as free radical scavengers using the DPPH radical scavenging assay. The results are presented in Table 4. The antioxidant capacity of SA films was significantly improved ($P \leq 0.05$) by adding PCO compared to the blank SA-based films, which recorded the lowest antioxidant activity. This result could be explained by the concentration of PCO extract in the SA matrix, which is directly correlated with the TPC content in plant extract, thereby increasing the antioxidant activity of biopolymer films [43]. The enhanced antiradical activity of the SA films enriched with PCO extract suggests that PCO is a potent antioxidant, as the high radical scavenging activity is related to the high content of ortho-dihydroxylated aromatic components such as hydroxytyrosol, tyrosol, verbascoside, oleuropein, and other compounds that serve as hydrogen donors and effectively scavenge the free radicals [55]. Comparable results have been documented in other polysaccharide-based films incorporating polyphenol extracts [56]. The excellent antioxidant activity exhibited by SA films enriched with PCO extract suggests their potential as promising

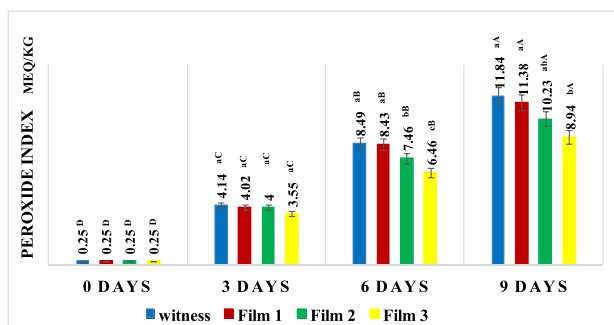


Fig. 4. Peroxide values of sunflower oil samples coated with films and the non-coated samples. Witness: Uncoated sunflower oil; Film 1: sunflower oil protected with pure SA film; Film 2: sunflower oil coated with composite SA film loaded 0.1% PCO; Film 3: sunflower oil coated with composite SA film loaded 0.2% PCO.

Table 4. Bioactive properties of the film samples.

Film sample	TPC ($\mu\text{g}\cdot\text{g}^{-1}$ film)	Antioxidant power	Antibacterial power « IZ (mm) »			
		% inhibition	<i>Echerichia coli</i>	<i>Salmonella enterica</i>	<i>Listeria monocytogenes</i>	<i>Staphylococcus aureus</i>
Film 1	64.37159 \pm 0.003 ^(b)	80.28 \pm 0.448 ^(b)	0.00(c)	0.00 \pm 0.5 ^(b)	0.00 \pm 0.5 ^(c)	0.00
Film 2	74.52147 \pm 0.002 ^(a)	98.04 \pm 0.448 ^(a)	14.6 \pm 0.5(b)	16.3 \pm 0.5 ^(a)	14.6 \pm 1.5 ^(b)	0.00
Film 3	80.26416 \pm 0.003 ^(a)	98.68 \pm 0.448 ^(a)	16 \pm 0.5(a)	17 \pm 0.00 ^(a)	19.6 \pm 0.5 ^(a)	0.00

TPC, total phenolic content. a-c: Lowercase letters within the same line refers to statistically significant differences ($P < 0.05$). Film 1: pure sodium alginate film; Film 2: sodium alginate films fitted with 0.1% of PCO; Film 3: sodium alginate film fitted with 0.2% of PCO.

packaging materials. These films could be used to improve shelf life and slow down the auto-oxidation process of foods, especially oxygen-sensitive foods.

3.13. Antimicrobial activity of films

Table 4, displays the antibacterial activities of alginate films with different concentrations of PCO extract. The control film showed no inhibitory effect against any of the studied microorganisms, consistent with the results documented by Zineb Mahcene et al. [57]. With the increase of PCO concentration in the film, the antimicrobial activity increased from 14.66 to 16 mm of *Echerichia coli* bacterial growth, from 12.66 to 19.66 mm of *L. monocytogenes* growth, and from 14.33 to 17 mm of *Salmonella enterica* growth, while no inhibition zone was observed for *S. aureus*, although the antimicrobial activity against *S. aureus* was found in the PCO extract. This discrepancy might be due to several factors, including the concentration of PCO in the film being too low to exhibit inhibitory effects compared to the extract alone. Additionally, some compounds may be less effective against *S. aureus*, possible interactions between the hydroxyl groups of phenolic compounds and the SA polymeric matrix, the rate at which the PCO extract is released from the alginate films, the film preparation method, and environmental conditions could also influence the observed results. Various bioactivities, including antimicrobial properties, have been attributed to olive mill wastewater [58]. The high content of biomolecules, specifically phenolic acids such as hydroxytyrosol, tyrosol, oleuropein, verbascoside, oleacein, or oleocanthal has been related to these properties, as stated by Ozcan and Matthaeus [59]. On the other hand, Gullón et al. [60] assert that attributing antibacterial properties to specific components becomes highly challenging when dealing with complex mixtures of bioactive compounds. In this sense, several authors have considered that interactions between bioactive components such as synergism, antagonistic, and chemical reactions as well as between these chemicals, and other elements, such as nutrients in the culture medium, are essentially causes of stronger

antimicrobial activity [61]. These results provide compelling evidence for the hypothesis that the release of phenolic compounds from PCO extract into the SA films is principally responsible for the increase in film activity. Phenolic compounds exert a significant influence on the structural and functional features of bacterial membranes through various processes, including protein denaturation, suppression of enzyme processes essential for microbial growth, and an elevation in cell membrane permeability. Consequently, these interactions result in the leakage of cytoplasmic contents, as explained by Gullón et al. [60].

4. Conclusion

This study highlights the valorization of olive mill wastewater, a cost-effective by-product of the olive industry, as a natural antioxidant source for developing active polymeric packaging materials for food applications. For the first time, the research demonstrates that active edible films can be successfully developed by incorporating different concentrations of PCO from olive waste into an alginate-based film. The effects of PCO addition on the physical-chemical, thermal, morphological, optical, barrier, and bioactive characteristics of alginate films and their biodegradability were studied. The findings indicated that adding PCO to the alginate film led to slightly increased film thickness and improved tensile strength properties. Furthermore, it enhanced thermal stability while reducing moisture content, WVP, and O2P values. It was obtained that this film is biodegradable. FTIR and SEM results confirmed that the interactions between the extract components and alginate chains, mainly through hydrogen bonding, were responsible for the observed effects of PCO. The PCO-enriched SA films demonstrated excellent light barrier properties, strong DPPH radical scavenging ability, and satisfactory antibacterial activity against foodborne bacteria. In general, alginate films incorporated with PCO exhibit promising potential in food packaging, particularly for products susceptible to lipids and for coating fresh-cut fruits and vegetables. However,

further experiments are required to examine the storage properties of food products coated with these films.

Ethics information

None.

Funding

No external funding received.

Acknowledgements

This study is for research purposes only, and it is clarified that no external funding was received, and no conflicts of interest declared by the authors. Also, we would like to extend our appreciation to Yildiz Technical University, Istanbul, Turkey, for their collaboration in facilitating this research.

References

- [1] P. Scarfato, L. Di Maio, L. Incarnato, Recent advances and migration issues in biodegradable polymers from renewable sources for food packaging, *J. Appl. Polym. Sci.* 132 (2015) 42597–42608, <https://doi.org/10.1002/app.42597>.
- [2] L.C. Paixão, I.A. Lopes, A.K.D. Barros Filho, A.A. Santana, Alginate biofilms plasticized with hydrophilic and hydrophobic plasticizers for application in food packaging, *J. Appl. Polym. Sci.* 136 (2019) 48263–48274, <https://doi.org/10.1002/app.48263>.
- [3] G. Nešić, Cabrera-Barjas, S. Dimitrijević-Branković, S. Davidović, N. Radovanović, C. Delattre, Prospect of polysaccharide-based materials as advanced food packaging, *Molecules* 25 (2019) 135–170, <https://doi.org/10.3390/molecules25010135>.
- [4] M. Nasrollahzadeh, M. Sajjadi, S. Irvani, R.S. Varma, Starch, cellulose, pectin, gum, alginate, chitin and chitosan derived (nano) materials for sustainable water treatment: a review, *Carbohydr. Polym.* 251 (2021) 116986–116999, <https://doi.org/10.1016/j.carbpol.2020.11698>.
- [5] B.J. Arroyo, A.C. Bezerra, L.L. Oliveira, S.J. Arroyo, E. A. de Melo, A.M.P. Santos, Antimicrobial active edible coating of alginate and chitosan add ZnO nanoparticles applied in guavas (*Psidium guajava*L.), *Food Chem.* 309 (2020) 12556–125586, <https://doi.org/10.1016/j.foodchem.2019.125566>.
- [6] Y. Wang, H. Du, M. Xie, G. Ma, W. Yang, Q. Hu, F. Pei, Characterization of the physical properties and biological activity of chitosan films grafted with gallic acid and caffeic acid: a comparison study, *Food Packag. Shelf Life* 22 (2019) 100401–100409, <https://doi.org/10.1016/j.fpsl.2019.100401>.
- [7] P. Umaraw, P.E.S. Munekata, A.K. Verma, F.J. Barba, V.P. Singh, P. Kumar, J.M. Lorenzo, Edible films/coating with tailored properties for active packaging of meat, fish and derived products, *Trends Food Sci. Technol.* 98 (2020) 10–24, <https://doi.org/10.1016/j.tifs.2020.01.032>.
- [8] C.L. Luchese, L.F.W. Brum, A. Piovesana, K. Caetano, S.H. Flores, Bioactive compounds incorporation into the production of functional biodegradable films- A review, *Polym. Renew. Resour.* 8 (2017) 151–176, <https://doi.org/10.1177/20412479170080040>.
- [9] S.A. Mir, B.N. Dar, A.A. Wani, M.A. Shah, Effect of plant extracts on the techno-functional properties of biodegradable packaging films, *Trends Food Sci. Technol.* 80 (2018) 141–154, <https://doi.org/10.1016/j.tifs.2018.08.004>.
- [10] A.C.P. Vital, A. Guerrero, M.G. Ornaghi, E.M.B.C. Kempinski, C. Sary, J. de O. Monteschio, I.N. do Prado, Quality and sensory acceptability of fish fillet (*Oreochromis niloticus*) with alginate-based coating containing essential oils, *J. Food Sci. Technol.* 55 (2018) 4945–4955, <https://doi.org/10.1007/s13197-018-3429-y>.
- [11] B. Zhang, Y. Liu, H. Wang, W. Liu, K. Cheong, B. Teng, Effect of sodium alginate- agar coating containing ginger essential oil on the shelf life and quality of beef, *Food Control* 130 (2021) 108216–108264, <https://doi.org/10.1016/j.foodcont.2021.108216>.
- [12] H. Aloui, A.R. Deshmukh, C. Khomlaem, B.S. Kim, Novel composite films based on sodium alginate and gallnut extract with enhanced antioxidant, antimicrobial, barrier and mechanical properties, *Food Hydrocolloid.* 113 (2021) 106508–106557, <https://doi.org/10.1016/j.foodhyd.2020.106508>.
- [13] J. Chen, A. Wu, M. Yang, Y. Ge, P. Pristijono, J. Li, H. Mi, Characterization of sodium alginate-based films incorporated with thymol for fresh-cut apple packaging, *Food Control* 126 (2021) 108063–108071, <https://doi.org/10.1016/j.foodcont.2021.108063>.
- [14] L. Dou, B. Li, K. Zhang, X. Chu, H. Hou, Physical properties and antioxidant activity of gelatin-sodium alginate edible films with tea polyphenols, *Int. J. Biol. Macromol.* 118 (2018) 1377–1383, <https://doi.org/10.1016/j.ijbiomac.2018.06.121>.
- [15] W. Zam, Effect of alginate and chitosan edible coating enriched with olive leaves extract on the shelf life of sweet cherries (*prunus avium* L.), *J. Food Qual.* 2019 (2019) 8192964–8192971, <https://doi.org/10.1155/2019/8192964>.
- [16] S.F. Ng, S.L. Tan, Development and in vitro assessment of alginate bilayer films containing the olive compound hydroxytyrosol as an alternative for topical chemotherapy, *Int. J. Pharm.* 495 (2015) 798–806, <https://doi.org/10.1016/j.ijpharm.2015.09.057>.
- [17] M. Niaounakis, C.P. Halvadakis, *Olive-mill Waste Management – Literature Review and Patent Survey*, second ed., 5, Elsevier, Amsterdam: London, 2006, pp. 1–498.
- [18] E.De Marco, M. Savarese, A. Paduano, R. Sacchi, Characterisation and fractionation of phenolic compounds extracted from olive mill wastewaters, *Food Chem.* 104 (2007) 858–867, <https://doi.org/10.1016/j.foodchem.2006.10.005>.
- [19] E. Capanoglu, J. Beekwilder, D. Boyacioglu, R. Hall, R. De Vos, Changes in antioxidant and metabolite profiles during production of tomato paste, *J. Agric. Food Chem.* 56 (2008) 964–973, <https://doi.org/10.1021/jf072990e>.
- [20] F. Tornuk, O. Sagdica, M. Hancerib, H. Yetim, Development of LLDE based active nanocomposite films with nanoclays impregnated with volatile compounds, *Food Res. Int.* 107 (2018) 337–345, <https://doi.org/10.1016/j.foodres.2018.02.036>.
- [21] E. M Ciannamea, J.P. Espinosa, P.M. Stefani, R.A. Ruseckaite, Long-term stability of compression-molded soybean protein concentrate films stored under specific conditions, *Food Chem.* 243 (2018) 448–452, <https://doi.org/10.1016/j.foodchem.2017.08.069>.
- [22] C. Liu, J. Huang, X. Zheng, S. Liu, K. Lu, K. Tang, J. Liu, Heat sealable soluble soybean polysaccharide/gelatin blend edible films for food packaging applications, *Food Packag. Shelf Life* 24 (2020) 100485–100494, <https://doi.org/10.1016/j.fpsl.2020.100485>.
- [23] S. Memiş, F. Tornuk, F. Bozkurt, M.Z. Durak, Production and characterization of a new biodegradable fenugreek seed gum based active nanocomposite film reinforced with nanoclays, *Int. J. Biol. Macromol.* 103 (2017) 669–675, <https://doi.org/10.1016/j.ijbiomac.2017.05.09>.
- [24] S. Park, Y. Zhao, Incorporation of a high concentration of mineral or vitamin into chitosan-based films, *J. Agric. Food Chem.* 52 (2004) 1933–1939, <https://doi.org/10.1021/jf034612p>.
- [25] ASTM International, Standard test method for tensile properties of thin plastic sheeting, in: *Annual Book of ASTM Standards* (Vol. 08.01), Standards Designations: D882-12, ASTM International, West Conshohocken, PA, USA, 2012, <https://doi.org/10.1520/D0882-12>.

- [26] S.D. Yoon, Y.M. Kim, B.I. Kim, J.Y. Je, Preparation and antibacterial activities of chitosan-gallic acid/polyvinyl alcohol blend film by LED-UV irradiation, *J. Photo Chem. Photobiol. B Biol.* 176 (2017) 145–149, <https://doi.org/10.1016/j.jphotobiol.2017.09.024>.
- [27] P.K. Dutta, S. ShipraTripathi, G.K. Mehrotra, j. Joydeep Dutta, Perspectives for chitosan based antimicrobial films in food applications, *Food Chem.* 114 (2009) 1173–1182, <https://doi.org/10.1016/j.foodchem.2008.11.047>.
- [28] M. Pérez-Bonilla, S. Salido, T.A. van Beek, J. Altarejos, Radical-scavenging compounds from olive tree (*Olea europaea* L.) wood, *J. Agric. Food Chem.* 62 (2013) 144–151, <https://doi.org/10.1021/jf403998t>.
- [29] G. Bisignano, A. Tomaino, R.L. Cascio, G. Crisafi, N. Uccella, A. Saija, On the in-vitro antimicrobial activity of oleuropein and hydroxytyrosol, *J. Pharm. Pharmacol.* 51 (1999) 971–974, <https://doi.org/10.1211/0022357991773258>.
- [30] I. Aissa, N. Kharrat, F. Aloui, M. Sellami, M. Bouaziz, Y. Gargouri, Valorization of antioxidants extracted from olive mill wastewater, *Biotechnol. Appl. Biochem.* 64 (2017) 579–589, <https://doi.org/10.1002/bab.1509>.
- [31] H. Akretche, G. Pierre, R. Moussaoui, P. Michaud, Delattre, cedric. Valorization of Olive mill wastewater for the development of biobased polymer films with antioxidant properties using eco-friendly processes, *Green Chem.* 21 (2019) 3065–3073, <https://doi.org/10.1039/c9gc00828d>.
- [32] A. Akcicek, F. Bozkurt, C. Akgül, S. Karasu, Encapsulation of olive pomace extract in rocket seed gum and chia seed gum nanoparticles: characterization, antioxidant activity and oxidative stability, *Foods* 10 (2021) 1735–1753, <https://doi.org/10.3390/foods10081735>.
- [33] H.K. Obied, M.S. Allen, D.R. Bedgood, P.D. Prenzler, K. Robards, R. Stockmann, Bioactivity and analysis of biophenols recovered from olive mill waste, *J. Agric. Food Chem.* 53 (2005) 823–837, <https://doi.org/10.1021/jf048569x>.
- [34] K. Khwaldia, Y. M'Rabet, A. Boulila, Active food packaging films from alginate and date palm pit extract: physicochemical properties, antioxidant capacity, and stability, *Food Sci. Nutr.* 11 (2022) 555–568, <https://doi.org/10.1002/fsn3.3093>.
- [35] M. Abdin, M.A. Salama, R. Gawad, M.A. Fathi, F. Alnadari, Two-steps of gelation system enhanced the stability of syzygium cumini anthocyanins by encapsulation with sodium alginate, maltodextrin, chitosan and gum Arabic, *J. Polym. Environ.* 29 (2021) 3679–3692, <https://doi.org/10.1007/s10924-021-02140-3>.
- [36] Y. Luo, H. Liu, S. Yang, J. Zeng, Z. Wu, Sodium alginate-based green packaging films functionalized by guava leaf extracts and their bioactivities, *Materials* 12 (2019) 2923–2938, <https://doi.org/10.3390/ma12182923>.
- [37] A. Augusto, J.R. Dias, M.J. Campos, N.M. Alves, R. Pedrosa, S.F.J. Silva, Influence of *Codium tomentosum* extract in the properties of alginate and chitosan edible films, *Foods* 7 (4) (2018) 53–66, <https://doi.org/10.3390/foods7040053>.
- [38] Pasukamonset, O. Kwon, S.A. Disakwattana, Alginate-based encapsulation of polyphenols from *Clitoria ternatea* petal flower extract enhances stability and biological activity under simulated gastrointestinal conditions, *Food Hydrocolloid.* 61 (2016) 772–779, <https://doi.org/10.1016/j.foodhyd.2016.06.03>.
- [39] L.M. Júnior, P.R. Rodrigues, R.G. da Silva, R.P. Vieira, R.M.V. Alves, Sustainable packaging films composed of sodium alginate and hydrolyzed collagen: preparation and characterization, *Food Bioproc. Technol.* 14 (2021) 2336–2346, <https://doi.org/10.1007/s11947-021-02727-7>.
- [40] W. Plazinski, A. Plazinska, Molecular dynamics study of the interactions between phenolic compounds and alginate/alginate acid chains, *New. J. Chem.* 35 (2011) 1607–1614, <https://doi.org/10.1039/C1NJ20273A>.
- [41] M. Moura-Alves, V.G. L Souza, J.A. Silva A. Esteves, L. M Pastrana, C. Saraiva, M.A. Cerqueira, Characterization of sodium alginate-based films Blended with olive leaf and laurel leaf extracts obtained by ultrasound-assisted technology, *Foods* 12 (2023) 4076–4096, <https://doi.org/10.3390/foods12224076>.
- [42] Y.L. Kuan, S.N. Sivasvaran, L.P. Pui, Y.A. Yusof, T. Senphan, Physicochemical properties of sodium alginate edible film incorporated with mulberry (*Morus australis*) leaf extract, *Pertanika J. Trop. Agric. Sci.* 43 (2020) 359–376.
- [43] J.G. de Oliveira Filho, J.M. Rodrigues, A.C.F. Valadares, A.B. de Almeida, T.M. de Lima, K.P. Takeuchi, C.C.F. Alves, H.A. de F. Sousa, E.R. da Silva, F.H. Dyszy, M.B. Egea, Active food packaging: alginate films with cottonseed protein hydrolysates, *Food Hydrocolloid.* 92 (2019) 267–275, <https://doi.org/10.1016/j.foodhyd.2019.01.05>.
- [44] J.T. Martins, M.A. Cerqueira, A.A. Vicente, Influence of atocopherol on physicochemical properties of chitosan-based films, *Food Hydrocolloid.* 27 (2012) 220–227, <https://doi.org/10.1016/j.foodhyd.2011.06.01>.
- [45] L.M. Júnior, P.R. Rodrigues, R.G. da Silva, R.P. Vieira, R.M.V. Alves, Sustainable packaging films composed of sodium alginate and hydrolyzed collagen: preparation and characterization, *Food Bioproc. Technol.* 14 (2021) 2336–2346, <https://doi.org/10.1016/j.fhfh.2022.100094>.
- [46] H. Li, C. Liu, J. Sun, S. Lv, Bioactive edible sodium alginate films incorporated with tannic acid as antimicrobial and antioxidative food packaging, *Foods* 11 (2022) 3044–3059, <https://doi.org/10.3390/foods11193044>.
- [47] E.M. Ciannamea, P.M. Stefani, R.A. Ruseckaite, Properties and antioxidant activity of soy protein concentrate films incorporated with red grape extract processed by casting and compression molding, *LWT-Food Sci. Technol.* 74 (2016) 353–362, <https://doi.org/10.1016/j.lwt.2016.07.073>.
- [48] H. Wu, Y. Lei, R. Zhu, M. Zhao, J. Lu, D. Xiao, C. Jiao, Z. Zhang, G. Shen, S. Li, Preparation and characterization of bioactive edible packaging films based on pomelo peel flours incorporating tea polyphenol, *Food Hydrocolloid.* 90 (2019) 41–49, <https://doi.org/10.1016/j.foodhyd.2018.12.01>.
- [49] C.M.P. Yoshida, V.B.V. Maciel, M.E.D. Mendonça, T.T. Franco, Chitosan biobased and intelligent films: monitoring pH variations, *LWT-Food Sci. Technol.* 55 (2014) 83–89, <https://doi.org/10.1016/j.lwt.2013.09.015>.
- [50] M.J. Costa, A.M. Marques, L.M. Pastrana, J.A. Teixeira, S.M. Sillankorva, M.A. Cerqueira, Physicochemical properties of alginate-based films: effect of ionic crosslinking and mannuronic and guluronic acid ratio, *Food Hydrocolloid.* 81 (2018) 442–448, <https://doi.org/10.1016/j.foodhyd.2018.03.01>.
- [51] R. Sothornvit, N. Pitak, Oxygen permeability and mechanical properties of banana films, *Food Res. Int.* 40 (2007) 365–370, <https://doi.org/10.1016/j.foodres.2006.10.010>.
- [52] M. Zubia, C. Payri, E. Deslandes, Alginate, mannitol, phenolic compounds and biological activities of two range-extending brown algae, *Sargassum mangarevense* and *Turbina ornata* (Phaeophyta: Fucales), from Tahiti (French Polynesia), *J. Appl. Phycol.* 20 (2008) 1033–1043, <https://doi.org/10.1007/s10811-007-9303-3>.
- [53] E. Koh, K.H. Hong, Gallnut extract-treated wool and cotton for developing green functional textiles, *Dyes Pigments* 103 (2014) 222–227, <https://doi.org/10.1016/j.dyepig.2013.09.015>.
- [54] L.G. Santos, G.F.A. Silva, B.M. Gomes, V.G. Martins, A novel sodium alginate active films functionalized with purple onion peel extract (*Allium cepa*), *Biocatal. Agric. Biotechnol.* 35 (2021) 102096–102102, <https://doi.org/10.1016/j.bcab.2021.102096>.
- [55] Z. Mahcene, A. Khelil, S. Hasni, P.K. Akman, F. Bozkurt, K. Birech, M.B. Goudjil, F. Tornuk, Development and characterization of sodium alginate based active edible films incorporated with essential oils of some medicinal plants, *Int. J. Biol. Macromol.* 145 (2020) 124–132, <https://doi.org/10.1016/j.ijbiomac.2019.12.093>.
- [56] J. Thielmann, S. Kohnen, C. Hauser, Antimicrobial activity of *Olea europaea* Linné extracts and their applicability as natural food preservative agents, *Int. J. Food Microbiol.* 251 (2017) 48–66, <https://doi.org/10.1016/j.ijfoodmicro.2017.03.019>.
- [57] Z. Mahcene, A. Khelil, S. Hasni, P.K. Akman, F. Bozkurt, K. Birech, M.B. Goudjil, F. Tornuk, Development and characterization of sodium alginate based active edible films incorporated with essential oils of some medicinal plants,

- Int. J. Biol. Macromol. 145 (2020) 124–132, <https://doi.org/10.1016/j.ijbiomac.2019.12.093>.
- [58] M.M. Özcan, B. Matthäus, A review: benefit and bioactive properties of olive (*Olea europaea* L.) leaves, *Eur. Food Res. Technol.* 243 (2016) 89–99, <https://doi.org/10.1007/s00217-016-2726-9>.
- [59] B. Gullón, P. Gullón, G. Eibes, C. Cara, A. De Torres, J.C. López-Linares, E. Ruiz, E. Castro, Valorization of olive agro-industrial by-products as a source of bioactive compounds, *Sci. Total Environ.* 645 (2018) 533–542, <https://doi.org/10.1016/j.scitotenv.2018.07.155>.
- [60] H.A. Hemeg, I.M. Moussa, S. Ibrahim, T.M. Dawoud, J.H. Alhaji, A.S. Mubarak, S.A. Kabli, R.A. Alsubki, A.M. Tawfik, S.A. Marouf, Antimicrobial effect of different herbal plant extracts against different microbial population, *Saudi J. Biol. Sci.* 27 (2020) 3221–3227, <https://doi.org/10.1016/j.sjbs.2020.08.015>.